

Correlations between IR Luminosity, Star Formation Rate, and CO Luminosity in the Local Universe

Matteo Bonato ^{1,2*}, Ivano Baronchelli ^{1,2}, Viviana Casasola ¹, Gianfranco De Zotti ³, Leonardo Trobbiani ^{1,4}, Erlis Ruli ⁵, Vidhi Tailor ^{1,4} and Simone Bianchi ⁶

¹ INAF—Istituto di Radioastronomia, Via Gobetti 101, I-40129 Bologna, Italy;

² Italian ALMA Regional Centre, Via Gobetti 101, I-40129 Bologna, Italy;

³ INAF—Osservatorio Astronomico di Padova, Vicolo dell’Osservatorio 5, I-35122 Padova, Italy;

⁴ Dipartimento di Fisica e Astronomia, Alma Mater Studiorum Università di Bologna, Via Piero Gobetti 93/2, I-40129 Bologna, Italy;

⁵ Dipartimento di Scienze Statistiche, Università degli Studi di Padova, Via Cesare Battisti 241/243, I-35121 Padova, Italy;

⁶ INAF—Osservatorio Astrofisico di Arcetri, Largo E. Fermi 5, 50125 Firenze, Italy.

* Correspondence: matteo.bonato@inaf.it

Abstract: We exploit the DustPedia sample of galaxies within approximately 40 Mpc, selecting 388 sources, to investigate the correlations between IR luminosity (L_{IR}), the star formation rate (SFR), and the CO(1-0) luminosity (L_{CO}) down to much lower luminosities than reached by previous analyses. We find a sub-linear dependence of the SFR on L_{IR} . Below $\log(L_{\text{IR}}/L_{\odot}) \simeq 10$ or $\text{SFR} \simeq 1 M_{\odot} \text{ yr}^{-1}$, the SFR/L_{IR} ratio substantially exceeds the standard ratio for dust-enshrouded star formation, and the difference increases with decreasing L_{IR} values. This implies that the effect of unobscured star formation overcomes that of dust heating by old stars, at variance with results based on the *Planck* ERCSC galaxy sample. We also find that the relations between the L_{CO} and L_{IR} or the SFR are consistent with those obtained at much higher luminosities.

Keywords: infrared; galaxies; star formation; statistics

1. Introduction

When the light emitted by young stellar populations is absorbed and re-emitted by dust, the total (8–1000 μm , rest frame) infrared (IR) luminosity, L_{IR} , is an effective measure of the star formation rate (SFR; [1]). These conditions are generally present in high-redshift, IR-luminous, dusty star-forming galaxies and in dense circum-nuclear starbursts at lower redshifts. However, in low- z disk and “normal” early-type galaxies the situation is more complicated. On the one hand, blue star-formation regions show that the light from young stars is at least partly unobscured. On the other hand, the IR emission shows a cold “cirrus” contribution, powered by the general interstellar radiation field, dominated by the old stellar population. The “cirrus” component may prevail especially in early-type galaxies. The two effects work in opposite directions and the result of their combination is largely unknown.

Dust luminosity has also been found to be a useful tracer of the molecular gas mass, alternative to the most commonly used CO(1-0) line (e.g., [2], and references therein). Molecular gas is the star-formation fuel; hence, it has a key role in galaxy evolution models. This has motivated investigations of correlations between the L_{IR} or the SFR and the L_{CO} ; however, these are limited to relatively high IR luminosity.

The complications mentioned above are particularly conspicuous at low IR luminosity/SFR. A preliminary investigation of the L_{IR} –SFR correlation in this regime was carried out by Clemens et al. [3]. They used a sample of 234 galaxies with flux density greater than 1.8 Jy at 545 GHz, located within approximately 100 Mpc (Negrello et al. [4]), drawn from the Planck Early Release Compact Source Catalogue (ERCSC; [5]). The distribution of their infrared luminosities peaked at $\log(L_{\text{IR}}/L_{\odot}) = 10$ with tails extending over the range $7.5 < \log(L_{\text{IR}}/L_{\odot}) < 12$.



Citation: Bonato, M.; Baronchelli, I.; Casasola, V.; De Zotti, G.; Trobbiani, L.; Ruli, E.; Tailor, V.; Bianchi, S.

Correlations between IR Luminosity, Star Formation Rate, and CO

Luminosity in the Local Universe.

Preprints 2024, 1, 0. <https://doi.org/>

Academic Editor: Oleg Malkov



Copyright: © 2024 by the authors. Licensee MDPI, Basel, Switzerland. This article is an open access article distributed under the terms and conditions of the Creative Commons Attribution (CC BY) license (<https://creativecommons.org/licenses/by/4.0/>).

In this paper, we exploit the DustPedia database¹, which allows us to explore the $L_{\text{IR}}\text{--SFR}$ relation down to the dust luminosity much fainter than that reached by the sample used by Clemens et al. [3]. It also allows us to investigate the correlation between L_{IR} and L_{CO} in this luminosity regime. The galaxies in the sample are morphologically classified so that it is possible to look for similarities and differences between early- and late-type populations.

The rest of this paper is structured as follows. Section 2 presents a short description of the sample. In Section 3, the $L_{\text{IR}}\text{--SFR}\text{--}L_{\text{CO}}$ correlations are analyzed and described. The main conclusions are presented in Section 4.

2. Data

DustPedia (Davies et al. [6]) is a large collaborative project aimed at substantially improving our understanding of the properties of dust in nearby galaxies and of its influence on physical processes occurring in the interstellar medium.

The DustPedia sample includes galaxies within a recession velocity of approximately 3000 km/s (corresponding to a distance of about 40 Mpc) and a major axis of the isophote at the optical surface brightness of $25 \text{ mag arcsec}^{-2}$, $D_{25} > 1'$. Galaxies were further required to be detected by the *Herschel* Space Telescope mission and to be brighter than the Wide-Field Infrared Survey Explore (WISE) $3.4 \mu\text{m}$ all-sky 5σ sensitivity limit.

The sample reaches $\log(L_{\text{IR}}/L_{\odot}) \lesssim 6.5$ and $\log(\text{SFR}/M_{\odot} \text{ yr}^{-1}) \lesssim -3$. Luminosities in the CO(1–0) line (L_{CO}) were collected from the literature and homogenized by Casasola et al. [7] [see their Table A.1, for the references of data sources]. The CO measurements are available for only $\sim 24\%$ of the sample and refer to late-type galaxies only. CO luminosities were computed using the distances in the DustPedia catalogue, which are redshift-independent in most cases and were otherwise computed using $h = H_0/100 \text{ km s}^{-1} \text{ Mpc}^{-1} = 0.73$.

The photometric DustPedia dataset consists of 875 galaxies for which multi-wavelength aperture-matched photometry for up to 41 bands, from far UV- to microwaves, was performed uniformly [8]. Nersesian et al. [9] dropped 61 galaxies with poor quality measurements in some bands or insufficient coverage of the spectral energy distribution (SED) from this dataset.

To the remaining 814 galaxies they applied the SED fitting Code Investigating GALaxy Emission (CIGALE; [10–12]), upgraded implementing The Heterogeneous Evolution Model for Interstellar Solids (THEMIS; [13,14]) dust model. Many DustPedia galaxies also belong to the Updated Nearby Galaxy Catalog, for which Karachentsev and Kaisina [15] derived SFR estimates from $H\alpha$ and UV measurements. We checked that such estimates are in very good agreement with the CIGALE's ones.

Through CIGALE, they derived the physical properties of each galaxy, including the stellar mass, the current SFR, the dust mass and temperature, and the total dust luminosity, L_{dust} (essentially equal to L_{IR}), with their uncertainties. They also investigated the dust heating by the old (age $> 200 \text{ Myr}$) and young ($\leq 200 \text{ Myr}$) stellar populations separately.

We further excluded the 19 galaxies for which the results could be biased by the presence of an AGN [16] (no AGN model was used in the fits) and the four galaxies which may have a substantial radio contribution to the far-infrared (FIR) to millimetre (mm) luminosity [9]. We were then left with 791 galaxies. A large fraction of them have a weak FIR to mm emission, so their total dust luminosity and SFR are highly uncertain. To avoid an excessive spread of the distribution of the SFR versus L_{IR} due to uncertainties, we limited our analysis to galaxies for which the estimates of each of these quantities are at least three times their respective uncertainties. This left 388 sources which constitute our final sample.

We consider two morphological classes, early-type galaxies (ETGs) and late-type galaxies (LTGs). We used the classification by Casasola et al. [7], which is based on de Vaucouleurs' [17] numerical type, T, complemented with additional criteria which affect a minor fraction of sources. The type T was taken from the HyperLEDA catalogue of

redshift-independent extragalactic distances (Makarov et al. [18]). ETGs include ellipticals and S0s, while LTGs comprise spirals and irregulars.

A table with classification, L_{IR} , SFR, $S_{\text{CO}(1-0)}$, and L_{CO} measurements for the sources of our final sample is provided as online Supplementary Material.

The distributions of the L_{IR} , SFR, and L_{CO} for our sample are shown in Figure 1. The peaks of the distributions are as follows: $L_{\text{IR}} \sim 5.99 \times 10^9$ (for the total and the late-type populations), $6.50 \times 10^8 L_{\odot}$ (for the early types); SFR ~ 0.94 (for the total and the late-type populations), $0.11 M_{\odot}/\text{yr}$ (for early types); and $L_{\text{CO}} \sim 6.94 \times 10^3 L_{\odot}$ (only a subsample of our late-type galaxies have CO measurements).

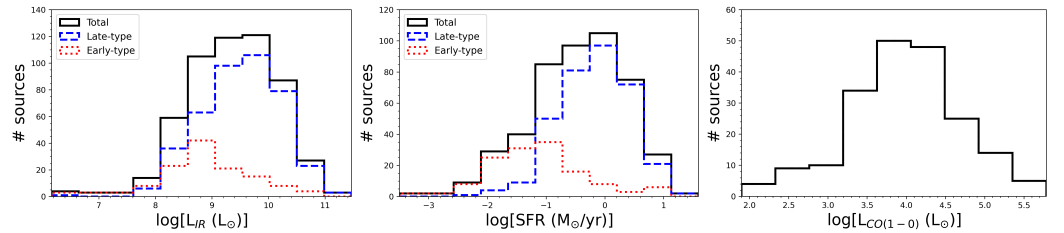


Figure 1. Distributions of $\log(L_{\text{IR}})$ (left), $\log(\text{SFR})$ (center), and $\log(L_{\text{CO}})$ (right) for our final sample: late-type galaxies (dashed blue lines), early-type galaxies (dotted red lines), and total (solid black lines). In the case of the distribution of $\log(L_{\text{CO}})$, only the total is shown; as mentioned in Section 1, CO(1-0) measurements are available for a subset of late-type galaxies only.

3. Results and Discussion

3.1. L_{IR} –SFR Correlation

The left and central panels of Figure 2 show the contributions, represented by the absorbed² starlight luminosity, L_{abs} , of old and young stellar populations to the total dust emission luminosity, L_{IR} . In the case of old stellar populations, the mean values of $\log(L_{\text{abs}}/L_{\text{IR}})$ for LTGs and ETGs are very close to each other, $\langle \log(L_{\text{abs}}/L_{\text{IR}}) \rangle \simeq -0.34 \pm 0.01$ and $\simeq -0.32 \pm 0.02$, respectively, corresponding to contributions of 46–48%. In some extreme cases, mostly associated with ETGs, dust heating is almost entirely due to old stars.

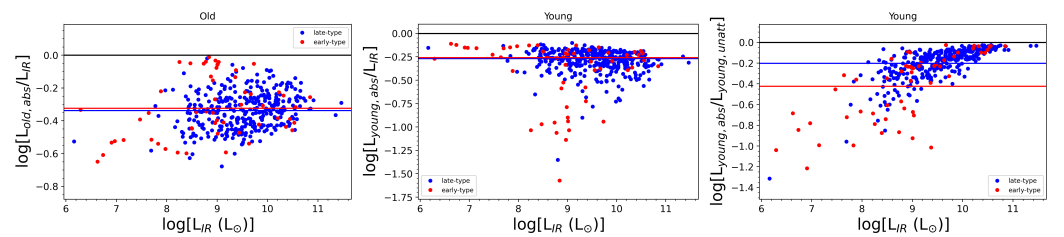


Figure 2. Ratio between the absorbed luminosity, L_{abs} , of old (left) and young (center) stellar populations and the total dust emission luminosity, L_{IR} . The right-hand panel shows the absorbed fraction of the starlight emitted by young stars, as a function of L_{IR} , for early- and late-type galaxies. The blue and red dots represent the late- and early-type galaxies, respectively; the horizontal blue and red lines correspond to the average values for the two galaxy types. The horizontal black line corresponds to unit ratios. We adopted the luminosities derived by Nersesian et al. [9] using CIGALE SED fitting.

Furthermore, in the case of the young stellar populations the median value of $\log(L_{\text{abs}}/L_{\text{IR}})$ is comparable for LTGs and ETGs, $\simeq -0.27 \pm 0.01$ and $\simeq -0.26 \pm 0.06$, respectively, corresponding to contributions to L_{IR} of $\simeq 54\%$ and $\simeq 55\%$, respectively. At the lowest IR luminosities ($\log(L_{\text{IR}}/L_{\odot}) \leq 8$), mostly associated with ETGs, dust heating is almost entirely due to young stars.

As expected, in LTGs the average contribution to dust heating of the young stellar population is larger than that of old stars, but the contribution of the latter is substantial. The same behavior is also shown by ETGs.

The right-hand panel of Figure 2 shows the dust-absorbed fraction of starlight emitted by young stellar populations in ETGs and LTGs as a function of the total IR luminosity. Such fraction is close to unity at high IR luminosity, but decreases, on average, with decreasing L_{IR} values. For $\log(L_{\text{IR}}/L_{\odot}) \leq 9$, more than half of the emission is unobscured, even for LTGs. The mean values of $\log(L_{\text{young,abs}}/L_{\text{young,unatt}})$ are -0.20 ± 0.01 for LTGs and -0.42 ± 0.04 for ETGs.

Figure 3 shows $\log(\text{SFR})$ versus $\log(L_{\text{IR}})$ for both early- and late-type galaxies (red and blue dots, respectively). We modeled the relation among the two quantities by means of a robust linear regression methodology³. In particular, the approach used is that of a robust M -estimator⁴. This methodology is implemented in the function *rlm* in the *R* package *MASS*.

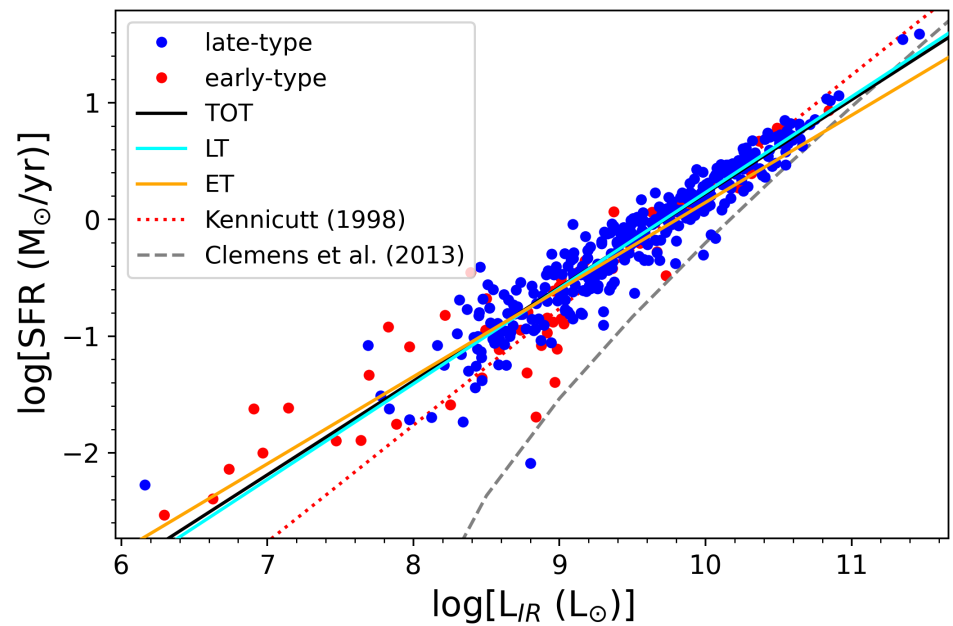


Figure 3. SFR versus L_{IR} for late- and early-type galaxies (blue and red dots, respectively). The solid cyan and orange lines show the best-fit relations for the two populations. The dotted red line shows the standard Kennicutt [1] relation. The dashed grey line shows the best-fit relation between SFR and *total* L_{IR} derived by Clemens et al. [3] for their sample. The typical uncertainties have a size close to those of data points.

In particular, we fitted a simple linear regression model,

$$\log(\text{SFR}_i) = \beta_0 + \beta_1 \log(L_{\text{IR},i}) + \epsilon_i, \quad (1)$$

where ϵ_i is the error term assumed to be identically and independently $N(0, \sigma^2)$ -distributed, $i = 1, \dots, n$.

The result for the total sample is

$$\log(\text{SFR}/M_{\odot} \text{ yr}^{-1}) = (-7.81 \pm 0.11) + (0.80 \pm 0.01) \times \log(L_{\text{IR}}/L_{\odot}), \quad (2)$$

where the uncertainties are the estimated standard errors (the robust confidence intervals at 95% confidence level for β_0 and β_1 are $[-8.03, -7.60]$ and $[0.78, 0.83]$, respectively).

For the late-type population, we obtained the following relation:

$$\log(\text{SFR}/M_{\odot} \text{ yr}^{-1}) = (-7.97 \pm 0.13) + (0.82 \pm 0.01) \times \log(L_{\text{IR}}/L_{\odot}). \quad (3)$$

The robust confidence intervals at a 95% confidence level for the intercept and the slope parameters are $[-8.21, -7.72]$ and $[0.79, 0.85]$, respectively.

For the early-type population, we obtained the following relation:

$$\log(\text{SFR}/M_{\odot}\text{yr}^{-1}) = (-7.32 \pm 0.34) + (0.75 \pm 0.04) \times \log(L_{\text{IR}}/L_{\odot}), \quad (4)$$

The robust confidence intervals at the 95% confidence level for the intercept and the slope parameters are $[-8.00, -6.65]$ and $[0.67, 0.82]$, respectively.

As illustrated by Figure 3, the best-fit relations for ETGs and LTGs are almost coincident. At medium to high luminosity, the relations agree with the standard Kennicutt [1] relation, which we chose in place of the more recent relation by Kennicutt and Evans [20] because it refers to the Salpeter initial mass function (IMF) also used for the DustPedia project⁵.

The increase in $\log(\text{SFR})$ with $\log(L_{\text{IR}})$ is sub-linear. At low luminosity, the SFRs estimated from CIGALE are substantially higher than expected from the Kennicutt [1] relation, implying that a large fraction of the light from young stars is not absorbed by dust, as also shown by Figure 2. In other words, using the IR luminosity alone and the Kennicutt [1] relation leads to underestimation of the SFR; a correct estimate requires taking into account both the absorbed and the unabsorbed light from young stars.

The data points are consistently above the best-fit relation between the SFR and total L_{IR} , the sum of the contributions of young and old stellar populations, derived by Clemens et al. [3] for their sample (dashed grey line). The different selection of the sample, the different resolution of the *Herschel* photometry used by DustPedia compared to the *Planck*'s used by Clemens et al. [3], and the fact that these authors used the preliminary photometry contained in the *Planck* ERCSC can have a role. We note, in particular, that ERCSC flux densities for extended galaxies, like those in the DustPedia sample, were found to be larger by substantial factors than the *Herschel* ones in nearby bands (see, e.g., [21]).

3.2. The $L_{\text{CO}}-L_{\text{IR}}$ and $L_{\text{CO}}-\text{SFR}$ Correlations

As stated in Section 1, we only have CO(1–0) measurements (provided as online Supplementary Material) for a subset of LTGs. We used the robust linear regression methodology described in Section 3.1 again to investigate the relation between L_{CO} and L_{IR} . We obtained the following:

$$\log L_{\text{CO}} = (-5.75 \pm 0.47) + (0.99 \pm 0.05) \times \log L_{\text{IR}}, \quad (5)$$

where both luminosities are in units of L_{\odot} . The robust confidence intervals at a 95% confidence level for the intercept and the slope are $[-7.29, -4.22]$ and $[0.84, 1.15]$, respectively.

The relation of Equation (5) is plotted against the data points in Figure 4, where relations found in the literature are also shown for comparison. Such relations are given in terms of L'_{CO} , in units of $[\text{K km s}^{-1} \text{pc}^2]$. We have the following [22,23]:

$$L_{\text{CO}} = 3.2 \times 10^{-11} \nu_r^3 L'_{\text{CO}}, \quad (6)$$

where the rest-frame frequency of the line, ν_r , is in GHz. For the CO(1-0) line, $\nu_r = 115.27$ GHz so that $\log L_{\text{CO}} = \log L'_{\text{CO}} - 4.31$.

The relations by Genzel et al. [24] and by Kamenetzky et al. [25] refer to the FIR luminosity between 50 and 300 μm and between 40 and 120 μm , respectively. We converted them to L_{IR} using $L_{\text{IR}}(8-1000 \mu\text{m})/L_{\text{FIR}}(50-300 \mu\text{m}) = 1.3$ and $L_{\text{IR}}(8-1000 \mu\text{m})/L_{\text{FIR}}(40-120 \mu\text{m}) = 1.7$ as suggested in those papers. Genzel et al. [24] derived two $L_{\text{FIR}}-L'_{\text{CO}}$ relations, referring to “all mergers” and to “all SFGs”, respectively. In Figure 4, we plot the “all SFGs” one.

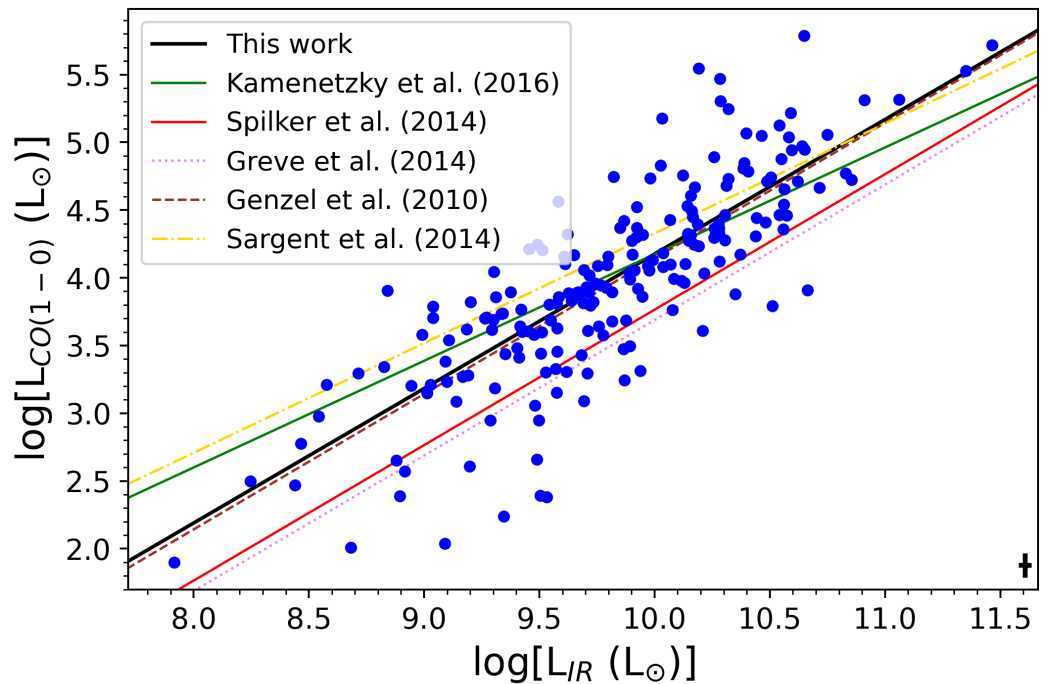


Figure 4. Relationship between $\log L_{\text{CO}}$ and $\log L_{\text{IR}}$. The black solid line represents the relation given by Equation (5). Five relations found in the literature are shown for comparison. In the bottom right corner, we show the median uncertainties of the plotted data points.

Our best-fit relationship is consistent with a linear relationship, in agreement with the results of Genzel et al. [24], Greve et al. [26], and Spilker et al. [27], based on samples at different redshifts and covering much higher luminosity ranges. Sub-linear relationships were found by Kamenetzky et al. [25] and Sargent et al. [28]. Our normalization is in close agreement with that of Genzel et al. [24] and somewhat higher, although consistent within the errors, with those of Greve et al. [26] and Spilker et al. [27].

Finally, we derived the relationship between $\log \text{SFR}$ and $\log L_{\text{CO}}$ for our sample using the same methodology. We obtained the following:

$$\log(L_{\text{CO}}/L_{\odot}) = (3.91 \pm 0.04) + (0.97 \pm 0.07) \times \log(\text{SFR}/M_{\odot}\text{yr}^{-1}). \quad (7)$$

The robust confidence intervals at a 95% confidence level for the intercept and the slope are [3.81,4.02] and [0.77,1.16], respectively. This relationship is shown in Figure 5, where those by Hunt et al. [29] and Gao and Solomon [30] are also shown for comparison.

The sample used by Gao and Solomon [30] includes 9 ultra-luminous, 22 luminous infrared galaxies (ULIRGs and LIRGs, respectively), and 34 normal spiral galaxies. The SFR was derived from the IR luminosity. Hunt et al. [29] measured the CO(1-0) luminosity of eight metal-poor dwarf galaxies; the SFR rate was computed from the $\text{H}\alpha$ and $24 \mu\text{m}$ luminosities. In both cases, the slope of the relation is consistent with unity, but metal-poor dwarf galaxies were found to have a lower CO luminosity at a given SFR by a factor of about 30. Our relationship is in good agreement, within the errors, with the one by Gao and Solomon.

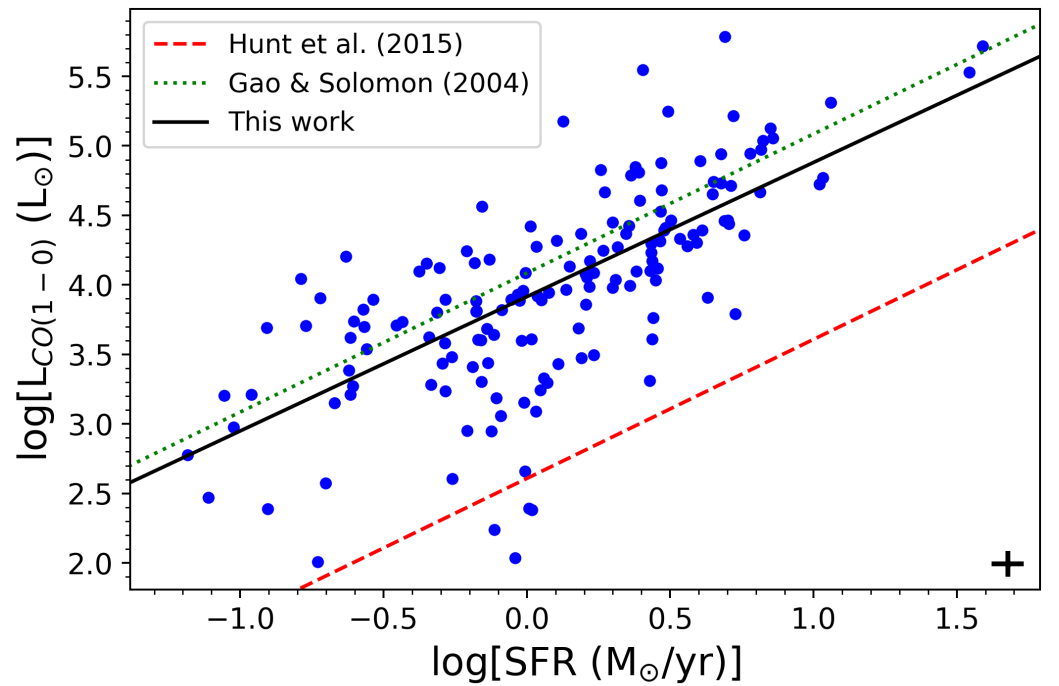


Figure 5. Relationship between $\log L_{\text{CO}}$ and $\log \text{SFR}$. The black solid line represents our relation defined by Equation (7). Shown also, for comparison, are the relationships by Gao and Solomon [30] and by Hunt et al. [29]. The Gao and Solomon [30] relationship was obtained using a sample including normal, luminous, and ultra-luminous infrared galaxies, while the sample of Hunt et al. [29] is made of metal-poor dwarf galaxies. The cross in the bottom-right corner represents the median uncertainties of the data points.

4. Conclusions

We investigated the correlations between the total (8–1000 μm) IR luminosity, the SFR, and the CO(1-0) luminosity for the DustPedia dataset of local galaxies defined by Nersesian et al. [9], removing the 23 galaxies showing either the presence of an AGN or a substantial non-thermal radio contribution to the IR luminosity. Furthermore, we limited our analysis to galaxies whose measurements of the L_{IR} and of the SFR have a signal-to-error ratio of at least three. Our final sample comprises 332 late-type and 56 early-type galaxies, i.e., a total of 388 sources.

The IR luminosity reaches $\log(L_{\text{IR}}/L_{\odot}) \lesssim 6.5$ and the SFR reaches $\log(\text{SFR}/M_{\odot} \text{ yr}^{-1}) \lesssim -3$, i.e., values at which L_{IR} is no longer expected to be a good proxy of the SFR. Nevertheless, the data show a statistically significant correlation between the two quantities down to the lowest luminosities and SFRs.

The relationship between the SFR and L_{IR} for our sample agrees with that by Kennicutt [1], which applies to complete absorption by dust of the light emitted by young stellar populations, above $\log(L_{\text{IR}}/L_{\odot}) \simeq 10$ or $\text{SFR} \simeq 1 M_{\odot} \text{ yr}^{-1}$. The slope is, however, significantly flatter, so our relation substantially exceeds the Kennicutt [1] one at low luminosity, implying that most of the starlight from young stars is not dust-absorbed. This is at variance with the results by Clemens et al. [3], based on a local sample drawn from the *Planck* ERCSC, which implies a dominant role, at low IR luminosity, of dust heating by old stars. Possible origins of the difference are pointed out.

Our sample allowed us to extend the relations between the CO(1-0) luminosity and the L_{IR} or the SFR to low luminosities. Their slopes and their normalizations turned out to be consistent with those obtained at much higher luminosities.

Supplementary Materials: A table with classification, L_{IR} , SFR, $S_{\text{CO}(1-0)}$, and L_{CO} measurements for the sources of our final sample is provided as online Supplementary Material.

Author Contributions: All authors have contributed substantially to the work reported. All authors have read and agreed to the published version of the manuscript.

Funding: M.B. and I.B. acknowledge support from INAF under the mini-grant “A systematic search for ultra-bright high-*z* strongly lensed galaxies in Planck catalogues”. V.C. and S.B. acknowledge support from INAF under the mini-grant “Face-to-Face with the Local Universe: ISM’s Empowerment”.

Data Availability Statement: The key data required to reproduce our analysis can be found in the online Supplementary Material.

Conflicts of Interest: The authors declare no conflicts of interest.

Notes

¹ <http://dustpedia.astro.noa.gr/>

² CIGALE, the SED fitting code employed by Nersesian et al. [9] on DustPedia galaxies, has the capability of disentangling attenuated and unattenuated emissions from old and young stellar populations. This enables us to quantify the fraction of energy absorbed by dust for each stellar component.

³ Robust linear regression down-weights extreme data points to obtain a more stable fit.

⁴ M-estimators are a class of estimators that extend the well-known maximum likelihood estimators (for further details, see Chapter 3 of [19]).

⁵ Please note that the Kennicutt and Evans [20] relation refers to the Kroupa IMF, which is very similar to the Chabrier IMF used by Clemens et al. [3]. Instead, the Kennicutt [1] relation and the Dustpedia fits refer to the Salpeter IMF. However, the difference is only a factor of 0.86 (Table 1 of Kennicutt and Evans [20]), meaning that the Kennicutt and Evans [20] calibration is lower (in SFR) than the Kennicutt [1] one by this factor. In Figure 3, for an appropriate comparison we chose to use the Kennicutt [1] relation and raise the Clemens et al. [3] relation by a factor of 1/0.86, which in practice brings everything to the Salpeter IMF. Alternatively, for an equally appropriate comparison, we could have lowered our SFRs by the factor of 0.86 and compared them to the Kennicutt and Evans [20] relation and the original Clemens et al. [3].

References

1. Kennicutt, R.C., Jr. The Global Schmidt Law in Star-forming Galaxies. *Astrophys. J.* **1998**, *498*, 541–552. <https://doi.org/10.1086/305588>.
2. Dunne, L.; Maddox, S.J.; Papadopoulos, P.P.; Ivison, R.J.; Gomez, H.L. Dust, CO, and [C I]: Cross-calibration of molecular gas mass tracers in metal-rich galaxies across cosmic time. *Mon. Not. R. Astron. Soc.* **2022**, *517*, 962–999. <https://doi.org/10.1093/mnras/stac2098>.
3. Clemens, M.S.; Negrello, M.; De Zotti, G.; Gonzalez-Nuevo, J.; Bonavera, L.; Cosco, G.; Guarese, G.; Boaretto, L.; Salucci, P.; Baccigalupi, C.; et al. Dust and star formation properties of a complete sample of local galaxies drawn from the Planck Early Release Compact Source Catalogue. *Mon. Not. R. Astron. Soc.* **2013**, *433*, 695–711. <https://doi.org/10.1093/mnras/stt760>.
4. Negrello, M.; Clemens, M.; Gonzalez-Nuevo, J.; De Zotti, G.; Bonavera, L.; Cosco, G.; Guarese, G.; Boaretto, L.; Serjeant, S.; Toffolatti, L.; et al. The local luminosity function of star-forming galaxies derived from the Planck Early Release Compact Source Catalogue. *Mon. Not. R. Astron. Soc.* **2013**, *429*, 1309–1323. <https://doi.org/10.1093/mnras/sts417>.
5. Planck Collaboration VII. Planck early results. VII. The Early Release Compact Source Catalogue. *Astron. Astrophys.* **2011**, *536*, A7. <https://doi.org/10.1051/0004-6361/201116474>.
6. Davies, J.I.; Baes, M.; Bianchi, S.; Jones, A.; Madden, S.; Xilouris, M.; Bocchio, M.; Casasola, V.; Cassara, L.; Clark, C.; et al. DustPedia: A Definitive Study of Cosmic Dust in the Local Universe. *Publ. Astron. Soc. Pac.* **2017**, *129*, 044102. <https://doi.org/10.1088/1538-3873/129/974/044102>.
7. Casasola, V.; Bianchi, S.; De Vis, P.; Magrini, L.; Corbelli, E.; Clark, C.J.R.; Fritz, J.; Nersesian, A.; Viaene, S.; Baes, M.; et al. The ISM scaling relations in DustPedia late-type galaxies: A benchmark study for the Local Universe. *Astron. Astrophys.* **2020**, *633*, A100. <https://doi.org/10.1051/0004-6361/201936665>.
8. Clark, C.J.R.; Verstocken, S.; Bianchi, S.; Fritz, J.; Viaene, S.; Smith, M.W.L.; Baes, M.; Casasola, V.; Cassara, L.P.; Davies, J.I.; et al. DustPedia: Multiwavelength photometry and imagery of 875 nearby galaxies in 42 ultraviolet-microwave bands. *Astron. Astrophys.* **2018**, *609*, A37. <https://doi.org/10.1051/0004-6361/201731419>.
9. Nersesian, A.; Xilouris, E.M.; Bianchi, S.; Galliano, F.; Jones, A.P.; Baes, M.; Casasola, V.; Cassarà, L.P.; Clark, C.J.R.; Davies, J.I.; et al. Old and young stellar populations in DustPedia galaxies and their role in dust heating. *Astron. Astrophys.* **2019**, *624*, A80. <https://doi.org/10.1051/0004-6361/201935118>.
10. Burgarella, D.; Buat, V.; Iglesias-Páramo, J. Star formation and dust attenuation properties in galaxies from a statistical ultraviolet-to-far-infrared analysis. *Mon. Not. R. Astron. Soc.* **2005**, *360*, 1413–1425. <https://doi.org/10.1111/j.1365-2966.2005.09131.x>.
11. Noll, S.; Burgarella, D.; Giovannoli, E.; Buat, V.; Marcellac, D.; Muñoz-Mateos, J.C. Analysis of galaxy spectral energy distributions from far-UV to far-IR with CIGALE: Studying a SINGS test sample. *Astron. Astrophys.* **2009**, *507*, 1793–1813. <https://doi.org/10.1051/0004-6361/200912497>.

12. Boquien, M.; Burgarella, D.; Roehlly, Y.; Buat, V.; Ciesla, L.; Corre, D.; Inoue, A.K.; Salas, H. CIGALE: A python Code Investigating GALaxy Emission. *Astron. Astrophys.* **2019**, *622*, A103. <https://doi.org/10.1051/0004-6361/201834156>.
13. Jones, A.P.; Fanciullo, L.; Köhler, M.; Verstraete, L.; Guillet, V.; Bocchio, M.; Ysard, N. The evolution of amorphous hydrocarbons in the ISM: Dust modelling from a new vantage point. *Astron. Astrophys.* **2013**, *558*, A62. <https://doi.org/10.1051/0004-6361/201321686>.
14. Jones, A.P.; Köhler, M.; Ysard, N.; Bocchio, M.; Verstraete, L. The global dust modelling framework THEMIS. *Astron. Astrophys.* **2017**, *602*, A46. <https://doi.org/10.1051/0004-6361/201630225>.
15. Karachentsev, I.D.; Kaisina, E.I. Star Formation Properties in the Local Volume Galaxies via H α and Far-ultraviolet Fluxes. *Astron. J.* **2013**, *146*, 46. <https://doi.org/10.1088/0004-6256/146/3/46>.
16. Bianchi, S.; De Vis, P.; Viaene, S.; Nersesian, A.; Mosenkov, A.V.; Xilouris, E.M.; Baes, M.; Casasola, V.; Cassarà, L.P.; Clark, C.J.R.; et al. Fraction of bolometric luminosity absorbed by dust in DustPedia galaxies. *Astron. Astrophys.* **2018**, *620*, A112. <https://doi.org/10.1051/0004-6361/201833699>.
17. de Vaucouleurs, G.; de Vaucouleurs, A.; Corwin, Herold G., J.; Buta, R.J.; Paturel, G.; Fouque, P. *Third Reference Catalogue of Bright Galaxies*; Springer: Berlin/Heidelberg, Germany, 1991.
18. Makarov, D.; Prugniel, P.; Terekhova, N.; Courtois, H.; Vauglin, I. HyperLEDA. III. The catalogue of extragalactic distances. *Astron. Astrophys.* **2014**, *570*, A13. <https://doi.org/10.1051/0004-6361/201423496>.
19. Huber, P.J.; Ronchetti, C.M. *Robust Statistics*; Wiley: Hoboken, NJ, USA, 2009.
20. Kennicutt, R.C.; Evans, N.J. Star Formation in the Milky Way and Nearby Galaxies. *Annu. Rev. Astron. Astrophys.* **2012**, *50*, 531–608. <https://doi.org/10.1146/annurev-astro-081811-125610>.
21. Herranz, D.; González-Nuevo, J.; Clements, D.L.; De Zotti, G.; Lopez-Caniego, M.; Lapi, A.; Rodighiero, G.; Danese, L.; Fu, H.; Cooray, A.; et al. Herschel-ATLAS: Planck sources in the phase 1 fields. *Astron. Astrophys.* **2013**, *549*, A31. <https://doi.org/10.1051/0004-6361/201219435>.
22. Solomon, P.M.; Downes, D.; Radford, S.J.E.; Barrett, J.W. The Molecular Interstellar Medium in Ultraluminous Infrared Galaxies. *Astrophys. J.* **1997**, *478*, 144–161. <https://doi.org/10.1086/303765>.
23. Carilli, C.L.; Walter, F. Cool Gas in High-Redshift Galaxies. *Annu. Rev. Astron. Astrophys.* **2013**, *51*, 105–161. <https://doi.org/10.1146/annurev-astro-082812-140953>.
24. Genzel, R.; Tacconi, L.J.; Gracia-Carpio, J.; Sternberg, A.; Cooper, M.C.; Shapiro, K.; Bolatto, A.; Bouché, N.; Bournaud, F.; Burkert, A.; et al. A study of the gas-star formation relation over cosmic time. *Mon. Not. R. Astron. Soc.* **2010**, *407*, 2091–2108. <https://doi.org/10.1111/j.1365-2966.2010.16969.x>.
25. Kamenetzky, J.; Rangwala, N.; Glenn, J.; Maloney, P.R.; Conley, A. L_{CO}/L_{FIR} Relations with CO Rotational Ladders of Galaxies Across the Herschel SPIRE Archive. *Astrophys. J.* **2016**, *829*, 93. <https://doi.org/10.3847/0004-637X/829/2/93>.
26. Greve, T.R.; Leonidaki, I.; Xilouris, E.M.; Weiß, A.; Zhang, Z.Y.; van der Werf, P.; Aalto, S.; Armus, L.; Díaz-Santos, T.; Evans, A.S.; et al. Star Formation Relations and CO Spectral Line Energy Distributions across the J-ladder and Redshift. *Astrophys. J.* **2014**, *794*, 142. <https://doi.org/10.1088/0004-637X/794/2/142>.
27. Spilker, J.S.; Marrone, D.P.; Aguirre, J.E.; Aravena, M.; Ashby, M.L.N.; Béthermin, M.; Bradford, C.M.; Bothwell, M.S.; Brodwin, M.; Carlstrom, J.E.; et al. The Rest-frame Submillimeter Spectrum of High-redshift, Dusty, Star-forming Galaxies. *Astrophys. J.* **2014**, *785*, 149. <https://doi.org/10.1088/0004-637X/785/2/149>.
28. Sargent, M.T.; Daddi, E.; Béthermin, M.; Aussel, H.; Magdis, G.; Hwang, H.S.; Juneau, S.; Elbaz, D.; da Cunha, E. Regularity Underlying Complexity: A Redshift-independent Description of the Continuous Variation of Galaxy-scale Molecular Gas Properties in the Mass-star Formation Rate Plane. *Astrophys. J.* **2014**, *793*, 19. <https://doi.org/10.1088/0004-637X/793/1/19>.
29. Hunt, L.K.; García-Burillo, S.; Casasola, V.; Caselli, P.; Combes, F.; Henkel, C.; Lundgren, A.; Maiolino, R.; Menten, K.M.; Testi, L.; et al. Molecular depletion times and the CO-to-H $_2$ conversion factor in metal-poor galaxies. *Astron. Astrophys.* **2015**, *583*, A114. <https://doi.org/10.1051/0004-6361/201526553>.
30. Gao, Y.; Solomon, P.M. The Star Formation Rate and Dense Molecular Gas in Galaxies. *Astrophys. J.* **2004**, *606*, 271–290. <https://doi.org/10.1086/382999>.

Disclaimer/Publisher’s Note: The statements, opinions and data contained in all publications are solely those of the individual author(s) and contributor(s) and not of MDPI and/or the editor(s). MDPI and/or the editor(s) disclaim responsibility for any injury to people or property resulting from any ideas, methods, instructions or products referred to in the content.